Supplemental Figures and Tables

Figure S1. Structural depictions of human PRC2, Related to Figure 1.

(A-C) Structural depictions of the EZH2-SRM/SET-I (A) and the EZH2-SRM/EED interfaces (B) and SAL (SET-activation loop) of EZH2 (C) in the presence of the JARID2-K116me3 peptide (amino acids 111-121), marked in orange (modified from PDB:5HYN). Note that the numbers of EZH2 residues were based on human EZH2 isoform a (751 amino acids).

(A and B) Residues that mediate interactions between the interfaces are highlighted.

(C) SAL (yellow) interacts with EED (green), SET domain of EZH2 (blue), and VEFS domain of SUZ12 (brown). The side chains of amino acids 116-121 in SAL are shown and PRC2 containing six alanine mutations at these residues, $EZH2^{(116\text{-}121)A}$, is catalytically inactive (see Figure 1).

Figure S2. PRC2 containing EZH2-SRM or EED anchoring mutants showed impaired responsiveness to H3K27me3 peptide for stimulated activity, but no defect in basal activity *in vitro*, Related to Figure 1.

(A) The purified recombinant PRC2 (EZH2, EED, SUZ12 and RBAP48) containing WT EZH2, EZH2-SRM activation-deficient mutants, EZH2 gain-of-function mutants, or EED anchoring mutants all form intact complexes. Proteins were detected by Coomassie blue staining of SDS-PAGE gels.

(B-D) Histone methyltransferase assay results with loading controls performed as in Figure 1C-1H. The levels of methylation on histone H3-containing oligonucleosomes are shown by autoradiography (top image). Coomassie blue staining of SDS-PAGE gels containing nucleosomes (middle image) or PRC2 components (bottom image) was used to visualize the relative concentration of each component present in each reaction.

(E) Structural modeling of EED anchorage mutants found in Weaver Syndrome. (i) Structural depiction of the EZH2-SRM/EED interface. Critical residues that mediate interactions are highlighted and the indicated distances between residues were measured using the Pymol program. (ii-iv) Structural modeling of EED^{R302G} (panel ii), EED^{R302S} (panel iii), or EED^{H258Y} (panel iv) is shown. EED^{R302G} and EED^{R302S} mutation may lose its interactions with $EZH2^{H129}$ and $EZH2^{H158}$. On the other hand, EED^{H258Y} mutation may cause steric collision with the main chain.

Figure S3. Analyses of PRC2 containing EZH2-SRM or EED anchoring mutants, Related to Figures 1 and 2.

(A) PRC2 containing $EZH2^{P132S}$ or $EZH2^{D136A}$ binds to the H3K27me3 peptide. Immunoprecipitation (IP) using a H3K27me3 peptide (amino acids 18-36) for the pull-

down of WT PRC2 or PRC2 containing EED^{Y365A}, EZH2^{P132S}, or EZH2^{D136A} mutants. Coomassie blue staining of input and IP samples separated on a SDS-PAGE gel is shown to visualize protein abundance. The EED cage mutant (EED^{Y365A}) manifested a binding defect to the peptide, whereas EZH2-SRM mutants (EZH2^{P132S} and EZH2^{D136A}) showed no defect.

(B) Quantitative histone mass-spectrometry analyses for endogenous H3K27 methylation levels in mESCs with the indicated genotypes. Global distribution of H3K27 methylation levels in E14 mESC cells including WT, EZH2-KO, and EZH2-KO cells rescued with EZH2^{WT} or EZH2-SRM mutants (left), and E14 mESC cells, including WT, EEDΔC-term, and EEDΔC-term cells rescued with EED^{WT} or EED anchoring mutants (right).

(C) The mESCs expressing PRC2/EED^{R302G} phenocopy the PRC2-deficiency phenotype of embryoid body (EB) differentiation. Western blot analysis of Brachyury, H3K27me3 and total histone H3 levels in WT or EEDΔC-term mESCs rescued with EED^{WT} or EED^{R302G} after 3 days of EB differentiation, as well as undifferentiated WT mESCs. Whole cell extract of mESCs was prepared as described in Materials and Methods. Brachyury was used as a mesodermal marker. EV, empty vector.

(D) EZH2-SRM mutants form intact complexes together with other PRC2 core subunits and accessory proteins *in vivo*. Immunoprecipitation (IP) using an anti-EZH2 monoclonal antibody (D2C9 Cell Signaling Technology) in WT and EZH2-KO E14 mESCs rescued with the indicated constructs. The mESC nuclear extract was prepared as described in Materials and Methods. Input and IP samples were separated on an SDS-PAGE gel. Western blot analysis for the PRC2 core subunits (EZH2, EED and SUZ12) and co-factors (JARID2 and AEBP2) is shown. Asterisk indicates a background band for the heavy chain of the antibody used in EZH2-IP. Total histone H3 was used as a loading control for input samples.

Figure S4. PRC2 containing EZH2^{L149Q} or EZH2^{Y153C} showed impaired responsiveness to H3K27me3 peptide for stimulated activity, but no defect in basal activity *in vitro*, and significantly reduced global H3K27me2/3 levels *in vivo*, Related to Figures 1 and 2.

(A) The purified recombinant PRC2 (EZH2, EED, SUZ12 and RBAP48) containing EZH2^{L149Q} or EZH2^{Y153C} forms intact complexes. Proteins were detected by Coomassie blue staining of SDS-PAGE gels.

(B and C) *Top*, HMT assays using wild-type (WT) PRC2 or PRC2 containing EZH2^{L149Q} or EZH2^{Y153C} (7.5, 15, or 30 nM) with unmodified oligonucleosomes (150 nM) as substrate in the absence (B) or increasing amounts of H3K27me3 peptide (0, 50, or 250 nM) (C). The levels of methylation on histone H3-containing oligonucleosomes are shown by autoradiography (top image). Coomassie blue staining of SDS-PAGE gels containing nucleosomes (middle image) or PRC2 components (bottom image) was used to visualize the relative concentration of each component present in each reaction. *Bottom*, Quantification of the relative amounts of ^{3}H-SAM incorporated into histone H3 after 60

min incubation of the assays. Data were plotted as Mean±SD (n=3 for each data point).

(D) Western blot analysis of EZH2, EED, H3K27me2, H3K27me3 and total histone H3 levels in E14 mESC cells, including WT, $EZH2^{-/-}$ (EZH2-KO), and EZH2-KO cells rescued with $EZH2^{WT}$, $EZH2^{L149Q}$, or $EZH2^{Y153C}$, as indicated. Gapdh was used as a loading control. mESC, mouse embryonic stem cells. EV, empty vector.

Figure S5. Targeting allosteric activation as an alternative strategy to inhibit PRC2, Related to Figures 4 and 6.

(A) The impact of EED^{R302G} on the allosteric activation of PRC2 overrides the gain-of-function effect of the $EZH2^{Y646N}$ mutation. Representative images for the HMT assays containing 500 nM WT PRC2 or PRC2 containing EED^{R302G}, $EZH2^{Y646N}$, or EED^{R302G} and $EZH2^{Y646N}$ in the absence or presence of the H3K27me3 peptide (500 or 2500 nM) using 150 nM of H3K27me2 oligonucleosomes as substrate. The levels of methylation on histone H3 are shown by autoradiography (top image). Coomassie blue staining of SDS-PAGE gels containing nucleosomes (middle image) or PRC2 components (bottom image) was used to visualize the relative concentration of each component present in each reaction. *Bottom*, quantification of the relative amounts of ^{3}H-SAM incorporated into histone H3. Data were plotted as Mean±SD (n=3 for each data point).

(B) WT PRC2 is intact in the presence of ADH-61 during allosteric activation. PRC2 (7.5 nM, total 2 µg) stimulated by the H3K27me3 peptide (150 nM) was incubated with or without ADH-61 (3.75 µM) in 1 ml of HMT buffer including 0.02 % NP-40 for 2 hr at 4 °C. PRC2 was pulled-down using an EZH2 monoclonal antibody. Input and IP samples were separated on an SDS-PAGE gel. Western blot analysis of EZH2, EED, SUZ12, and RBAP48 is shown.

(C) PRC2 containing EZH2-SRM mutants are intact in the presence of ADH-61 during allosteric activation. Representative HMT assays with 7.5 nM PRC2 comprising EZH2-SRM mutants in the presence of the H3K27me3 peptide (150 nM), with increasing amounts (0.75, 1.5 or 3.75 µM) of ADH-61 using unmodified oligonucleosomes (150 nM) as substrate. Details of the HMT assay conditions are described in Materials & Methods. Autoradiographic images indicate the levels of methylation on histone H3 (top) and Coomassie blue staining of SDS-PAGE gels shows histones (middle) or PRC2 components (bottom).

Figure S6. The EZH2-SRM/SET-I interface and the EZH2-SRM/EED anchorage contain groove surface features, Related to Figures 1 and 6.

(A-B) Surface representation of EZH2-SRM (pink)/SET-I (blue) interface. The positions of D142, F145, and P132 of EZH2 are highlighted in red. The groove surfaces are indicated by black arrows.

(C) Structural animation of EED. The positions of R236, H258, and R302 of EED are highlighted in dark grey. The groove feature generated by R236, H258, and R302 of EED is indicated by a black arrow.

(D) Surface representation of EZH2-SRM (red)/EED (grey) anchorage. H129 and H158 of EZH2 are highlighted in pink, and R236 and R302 of EED are highlighted in dark grey. (modified from PDB:5HYN)

Table S1. Mutations within EZH2-SRM/SET-I and EZH2-SRM/EED interfaces found in human cancers and Weaver syndrome, Related to Figures 1 and 2. The EZH2 and EED mutations used in this study are highlighted in red.

Table S2. The sequence of guide RNA, Template DNA for guide RNA and primers for CRISPR/Cas9 mediated genome editing, Related to Figure 2.

Supplemental Figures and Tables

Figure S1

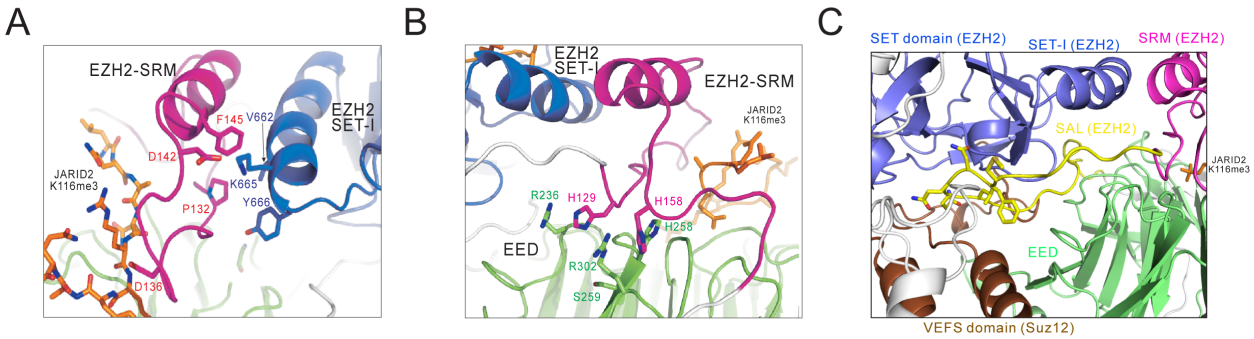

Figure S2

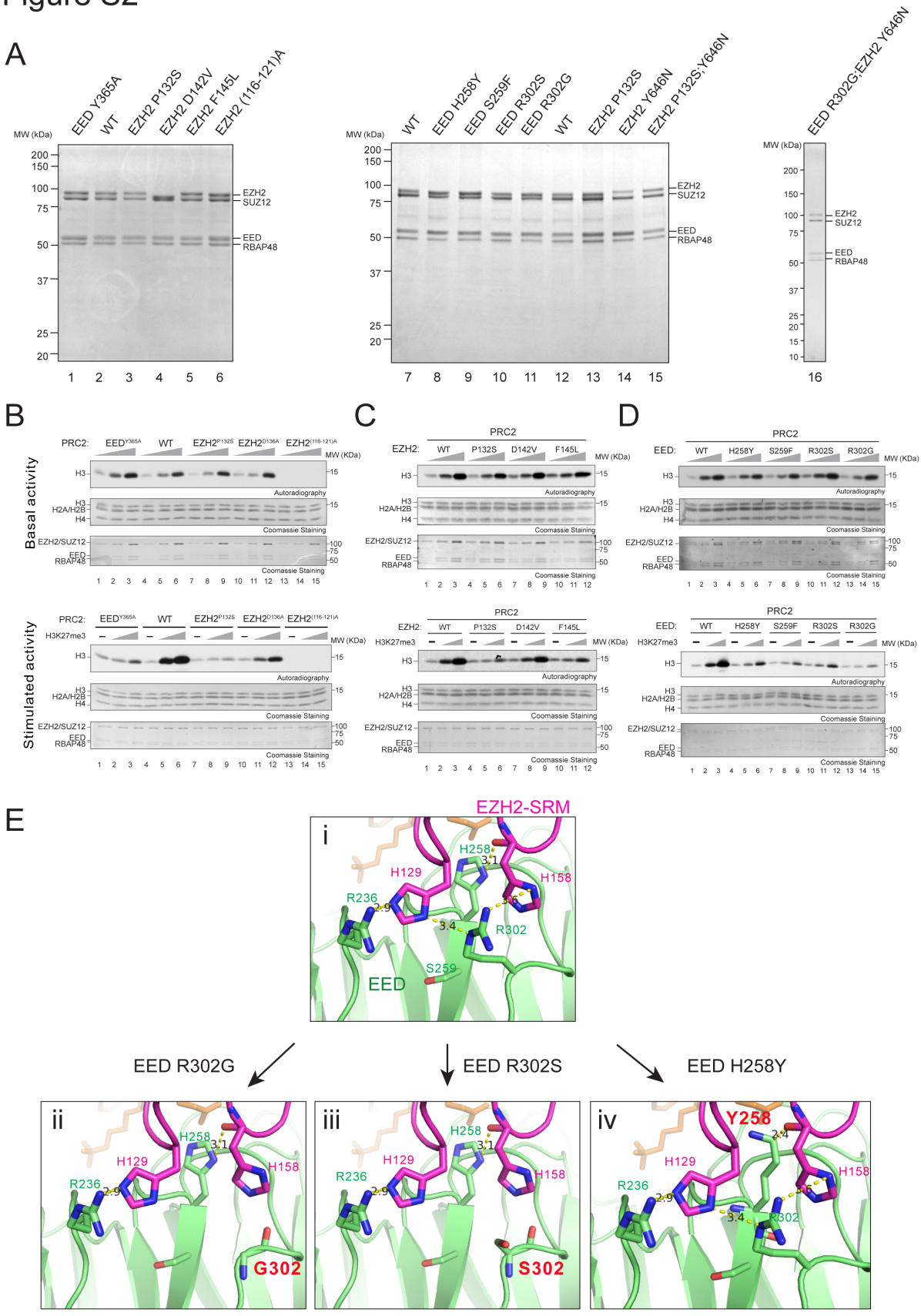
A
EED Y365A
WT
EZH2 P132S
EZH2 D142V
EZH2 F145L
EZH2 (116-121)A
MW (kDa)
EZH2
SUZ12
EED
RBAP48
WT
EED H258Y
EED S259F
EED R302S
EED R302G
WT
EZH2 P132S
EZH2 Y646N
EZH2 P132S;Y646N
EED R302G;EZH2 Y646N
B
C
D
PRC2:
EZH2:
EED:
Basal activity
Stimulated activity
H3K27me3
Autoradiography
Coomassie Staining
E
EZH2-SRM
i
H258
H129
H158
R236
R302
S259
EED
EED R302G
EED R302S
EED H258Y
ii
iii
iv
G302
S302
Y258

Figure S3

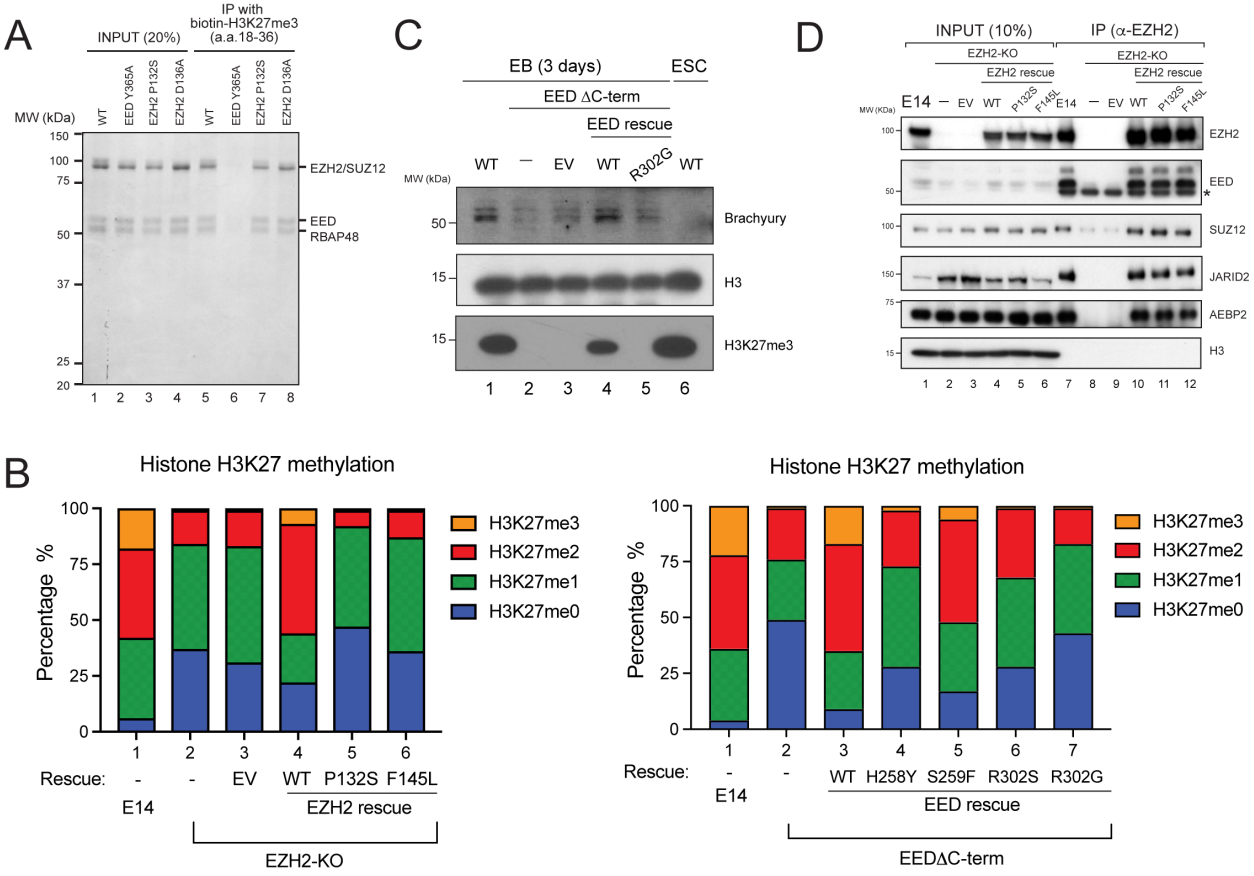
A
INPUT (20%)
IP with biotin-H3K27me3 (a.a.18-36)
WT
EED Y365A
EZH2 P132S
EZH2 D136A
MW (kDa)
EZH2/SUZ12
EED
RBAP48
C
EB (3 days)
ESC
EED ΔC-term
EED rescue
WT
EV
R302G
Brachyury
H3
H3K27me3
D
INPUT (10%)
IP (α-EZH2)
EZH2-KO
EZH2 rescue
E14
EZH2
EED
SUZ12
JARID2
AEBP2
H3
B
Histone H3K27 methylation
Percentage %
H3K27me3
H3K27me2
H3K27me1
H3K27me0
Rescue:
E14
EV
P132S
F145L
EZH2 rescue
EZH2-KO
H258Y
S259F
R302S
R302G
EED rescue
EEDΔC-term

Figure S4

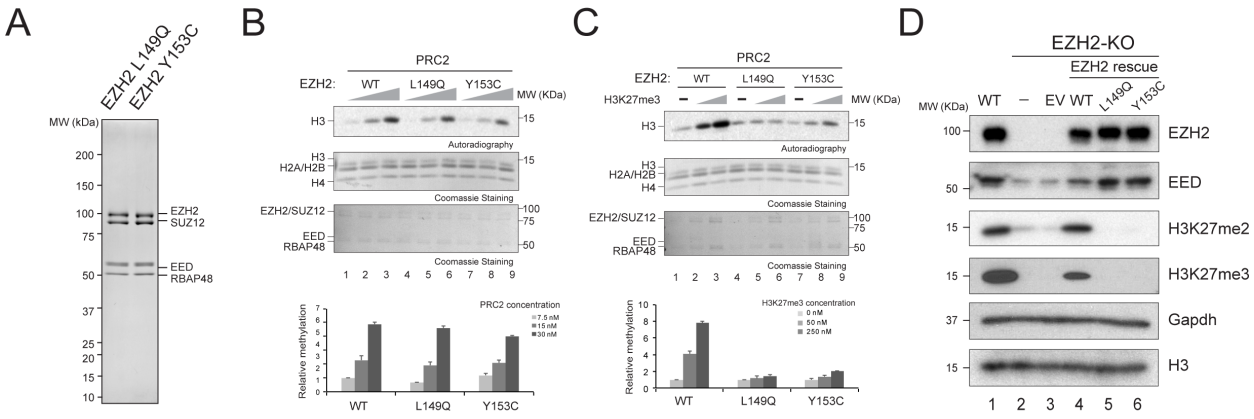
A
EZH2 L149Q
EZH2 Y153C
MW (kDa)
200
150
100
75
50
37
25
20
15
10
EZH2
SUZ12
EED
RBAP48
B
PRC2
EZH2:
WT
L149Q
Y153C
MW (KDa)
H3
Autoradiography
H3
H2A/H2B
H4
Coomassie Staining
EZH2/SUZ12
EED
RBAP48
Coomassie Staining
1 2 3 4 5 6 7 8 9
PRC2 concentration
7.5 nM
15 nM
30 nM
Relative methylation
WT
L149Q
Y153C
C
PRC2
EZH2:
WT
L149Q
Y153C
H3K27me3
MW (KDa)
H3
Autoradiography
H3
H2A/H2B
H4
Coomassie Staining
EZH2/SUZ12
EED
RBAP48
Coomassie Staining
1 2 3 4 5 6 7 8 9
H3K27me3 concentration
0 nM
50 nM
250 nM
Relative methylation
WT
L149Q
Y153C
D
EZH2-KO
EZH2 rescue
MW (KDa)
WT
–
EV
WT
L149Q
Y153C
EZH2
EED
H3K27me2
H3K27me3
Gapdh
H3
1 2 3 4 5 6

Figure S5

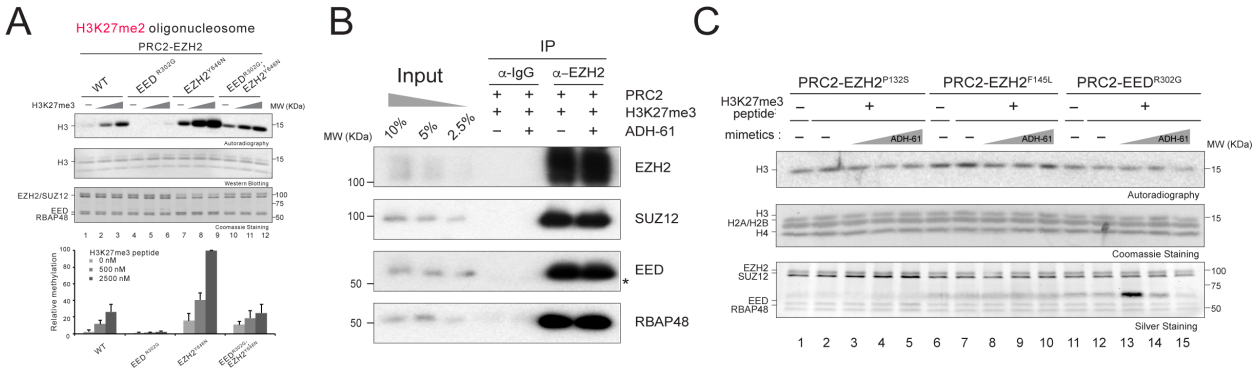
A
H3K27me2 oligonucleosome
PRC2-EZH2
WT
EED R302G
EZH2 Y646N
EED R302G EZH2 Y646N
H3K27me3
MW (KDa)
H3
Autoradiography
Western Blotting
EZH2/SUZ12
EED
RBAP48
Coomassie Staining
H3K27me3 peptide
0 nM
500 nM
2500 nM
Relative methylation
B
Input
IP
α-IgG
α-EZH2
10%
5%
2.5%
PRC2
H3K27me3
ADH-61
EZH2
SUZ12
EED
RBAP48
C
PRC2-EZH2 P132S
PRC2-EZH2 F145L
PRC2-EED R302G
H3K27me3 peptide
mimetics :
ADH-61
H3
H2A/H2B
H4
Autoradiography
Coomassie Staining
Silver Staining

Figure S6

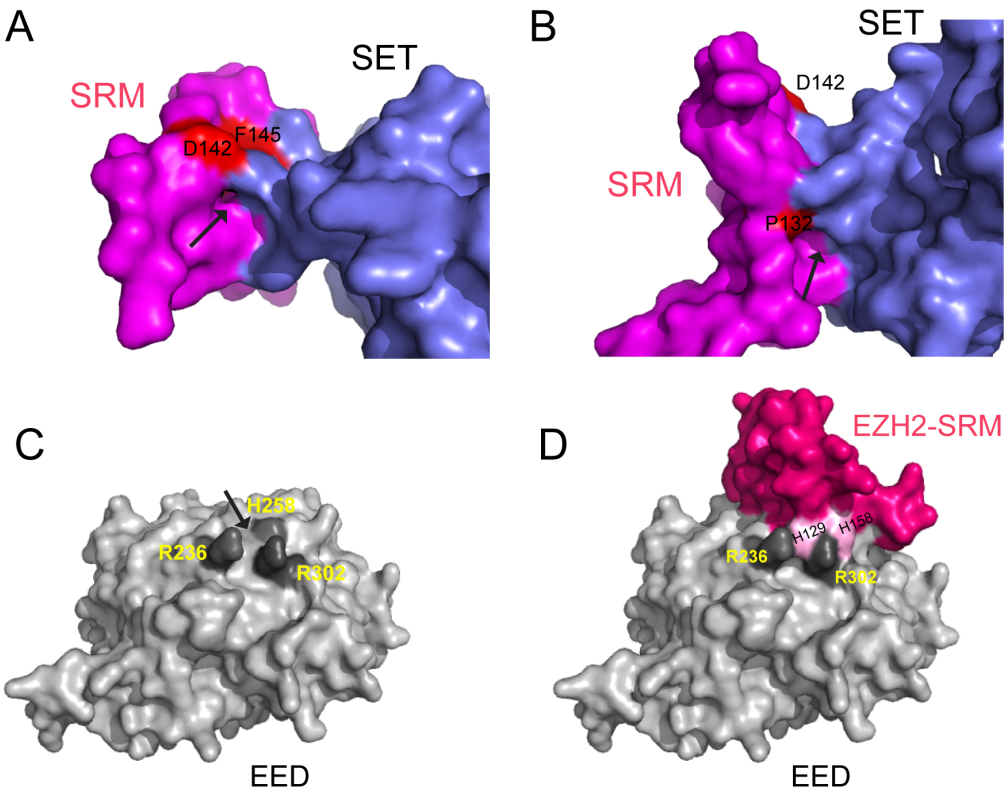
A
SET
SRM
F145
D142
B
SET
D142
SRM
P132
C
H258
R236
R302
EED
D
EZH2-SRM
H129
H158
R236
R302
EED

Table S1

Subunit	Diseases		Mutations
EZH2-SRM	Weaver Syndrome		N130K P132S Y133C M134T F145L E148L E148G Y153S Y153del K156E G159R
	Cancer	Melanoma	P132S D142V
		Acute myeloid Leukemia	H128R I131N I131F Y133N Y153C G155R G159R
		acute lymphoblastic leukemia	H128Q Y133H F145L G159R
		myelofibrosis (bone marrow cancer)	P132S G135R F145C F145S L149P L149Q I150T
		Myelodysplastic syndrome	I146N Y153C
		Bladder Urothelial Carcinoma	F145Y
		Colon adenocarcinoma	K151Q
EED anchoring	Weaver Syndrome		R236T H258Y R302G R302S
	Cancer	acute lymphoblastic leukemia	S259F
	other diseases	myeloproliferative neoplasms	R302G

Table S2

gRNA		
gRNA name;	**Sequence;**	**Experiment**
EZH2 KO	GGTTAACACAAAGCCCTGGA	EZH2-KO mESCs
EZH2 P132S to WT	GATGAAGTTTTAGATCAGGA	Melanoma COLO-679 reverse CRISPR (EZH2_P132S/WT to EZH2_WT/WT)
Template DNA for guide RNA		
gBlock name;	**Sequence;**	**Experiment**
EZH2 KO	TGTACAAAAAAGCAGGCTTTAAAGGAACCAATTCAGTCGACTGGATCCGGTACCAAGGTCGGGCAGGAAGAGGGCC TATTTCCCATGATTCCTTCATATTTGCATATACGATACAAGGCTGTTAGAGAGATAATTAGAATTAATTTGACTGTAAA CACAAAGATATTAGTACAAAATACGTGACGTAGAAAGTAATAATTTCTTGGGTAGTTTGCAGTTTTAAAATTATGTTTT AAAATGGACTATCATATGCTTACCGTAACTTGAAAGTATTTCGATTTCTTGGCTTTATATATCTTGTGGAAAGGACGAA ACACCGAATCTGACAAATCCGGCATGTTTTAGAGCTAGAAATAGCAAGTTAAAATAAGGCTAGTCCGTTATCAACTTG AAAAAGTGGCACCGAGTCGGTGCTTTTTTTCTAGACCCAGC TTTCTTGTACAAAGTTGGCATTA	EZH2-KO mESCs
EZH2 P132S to WT	TCACATTTGATACTTAGAGTAAACCTGCTTTTTAAATATATTTTTTTCTTTTAGGTGGAAGATGAAACTGTTTTACATAA CATTCCTTATATGGGAGATGAAGTTTTAGATCAGGATGGTACTTTCATTGAAGAACTAATAAAAAATTATGATGGGAA AGTACACGGGGATAGAGGTGAGCCATATGCTTCTTCTCTTGG	Melanoma COLO-679 reverse CRISPR (EZH2_P132S/WT to EZH2_WT/WT)
qPCR for validation		
primer name;	**Sequence;**	**Experiment**
Ezh2_left_arm_gPCR_F1	GGTTAACACAAAGCCCTGGA	EZH2-KO mESCs
Ezh2_left_arm_gPCR_R1	TGCCAGATCTGCAACCAATA	EZH2-KO mESCs
Ezh2_right_arm_gPCR_F1	TGGTGAATGGCAGTCTGTGT	EZH2-KO mESCs
Ezh2_right_arm_gPCR_R1	CCTTCCACCACCAAGAAAGA	EZH2-KO mESCs